Shoreline Retreat Forecasting due to Climate Change in the North Stradbroke Island, Australia

Muhamad Iqbal Januadi[1, 2], Evelyn Alicia Gomez Juarez[1]

[1] School of Earth and Environmental Science, University of Queensland, Australia.
[2] Department of Geography, Universitas Indonesia , Indonesia.

[a)] muhamad.iqbal41@sci.ui.ac.id, [b)] e.gomezjuarez@uq.net.au

Abstract. Coastal areas are important for humans but climate change increases current hazards such as sea level rise, inundation, coastal erosion, and shoreline retreat. Particularly, evaluation of potential consequences of coastal erosion and shoreline recession as a result of sea level rise should be undertaken. This study aims to i) assess the future shoreline retreat of a sub-tropical beaches in The North Stradbroke Island (NSI) by using a combination of observations and numerical modelling approaches and; ii) investigate the vulnerability of the coast by combing qualitative and qualitative assessments of coastal hazards and the location of coastal infrastructure. The effect of sea-level rise on shoreline recession is estimated using Bruun Rule and simulated under the sea-level rise by 2100, while the vulnerability assessment is undertaken using Coastal Vulnerability Index (CVI). The result shows that Frenchmans and Cylinder Beaches experience the highest total shoreline retreat in cases of 50% and 1% of exceedance. Meanwhile, the CVI results in the high score vulnerability in Home and Cylinder Beach, corresponding the human settlement location in this area.

Keywords: Bruun rule, climate change**,** GIS, shoreline retreat

1. Introduction

The coastal area has been considered as an important area for human being, and many people have lived within this area due to the tourism, economic value, natural resources, transportation, and ecological value (Mehvar et al., 2018). However, climate change threatens this system and causes various coastal hazards, such as coastal erosion and shoreline retreat (Saravanan et al., 2019). Shoreline erosion and recession due to the sea level rise are severe problems for coastal communities, and evaluation of possible impact caused by these events should be undertaken (Yoshida et al., 2014). Predicting shoreline recession, change, and vulnerability is a critical scientific action for policy and managers to avoid the disastrous impact in the future (Cooper & Pilkey, 2014).

Many papers have undertaken future shoreline recession prediction as essential information for coastal vulnerability assessment (Yoshida et al., 2014; Kinsela et al., 2016).

However, there is less information available for the shoreline change prediction and its vulnerability in North Stradbroke Island (NSI). In fact, this island has unique ecological value, high tourism prospect, and high indigenous value (Cox et al., 2011). The coastal hazards make these values would be threatened in the future and make this future prediction necessary. Therefore, forecasting the future shoreline retreat in NSI beaches would be very essential.

This project aims to predict the future shoreline recession and assess the coastal hazards vulnerability in NSI beach. To answer this aim, three main steps are undertaken: i) shoreline mapping, ii) shoreline recession prediction, iii) coastal vulnerability assessment. The effect of sea-level rise on shoreline recession is estimated using *Bruun Rule* (Yoshida et al., 2014) and simulated under the sea-level rise by 2100. Unlike the previous research, this study also will explain the effect of the headland bypassing process for the beach morphodynamics in NSI and propose the vulnerability index for each beach due to the coastal hazards. This information will be helpful for the marine scientist, engineer, and manager plan the strategic action for future beach system protection.

2. Study Site

The project focused on six areas in the northeast of North Stradbroke Island (NSI), Australia, also called *Minjerriba* (**Figure 1**). These are Flinders Beach, Home Beach, Cylinder Beach, Deadmans Beach, Frenchmans Beach, and Main Beach, and are located in the northeast of the island. NSI is an island of 275 km^2 made of sand, with a length of 37 km north-south and width of 11 km west-east. The topography is dominated by extensive sand dunes made of siliceous sands (Cox et al., 2011) and broad embayments and bedrock headlands are key features of the coastline, which have influence in beach morphodynamics (Whitlow, 2000).

Figure 1. Regional setting area of this project. (a) This project is undertaken in the north part of Northern Stradbroke Island. (b) The wave system in Northern Stradbroke Island which dominated by southeast wave and Hs 1.6 -1.8 m

There are six dominant soil types on the island; siliceous sand, podzols, acid peat, saline mud, red earth, and lithosols, that are present in eleven soil landscapes. The dominant vegetation communities are open eucalypt forest and woodland with grassy and heath vegetation and fringing wetlands that include wet-heathland, saltmarshes, sedge lands and open woodlands. Near to 20% of the island comprises fringing wetlands and beaches (Cox et al., 2011). Current sand beaches form the margins of the island on the north and east coasts. Behind them are located freshwater wetlands at the base of the dunes and the main groundwater reservoir. These beaches are dominated by wave action and northward sediment transport along the ocean (Cox et al., 2011; DERM, 2011).

NSI is located in a wave dominated environment of high-energy, whose currents are generated from east to southerly winds (DERM, 2011). These conditions cause differences in wave height (*Hs*) across the coast, being the southeast and east parts of the island those with higher wave heights (1.5-1.8 m.), whereas the north and west parts have lower heights with values of 1.4-1.5 m and 0.33 m, respectively (**Figure 1**). Also, wave period (*T*) is variable across the island. In the eastern and northern parts ranges from 7-8 s, while in the west is from 4-7 s. Most of the cyclones that cross Queensland, stay in the norther side, but in some occasions they move to the south, crating high waves due to heavy winds (DERM, 2011).

In addition, the beach within this island is also affected by the storm (**Figure 2**). The highest storm frequency occurred by 1990, with about 800 storms affected this area. It was observed that wave height increased proportionally to the duration of storms across the period analyzed.

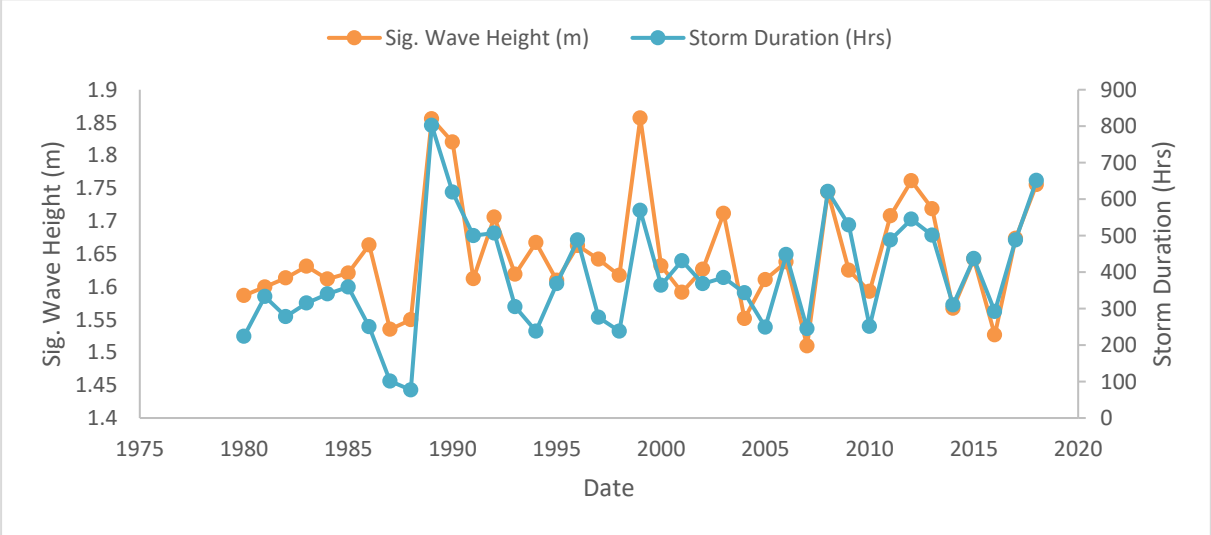

Figure 2. Significant wave height and annual storm duration for the period 1980-2018. The historical record was obtained from the Brisbane Wave Rider buoy, located off the coast of North Stradbroke Island.

3. Methodology

Shoreline Change Assessment

The shoreline changes vary over temporal and spatial scale and link to the accretion and erosion caused by the wave as the primary source of energy in the coastal zone (Masselink et al., 2011; Saravanan et al., 2019; Burningham & Miriam, 2020). In this study, the shoreline change position in the North Stradbroke coast is monitored for 60 years (1958-2018) using multi dated satellite images. Each time, the shoreline position is delineated using the high water line approximation (Burningham & Miriam, 2020) and use the shoreline position in 1958 as a base. The shoreline map from various year will be analysed using the Shorline Change Envelope (SCE), representing the total change and movement of shoreline position towards the baseline (de Bour et al., 2018). In addition, the trend of changing in each beach also is analysed using a simple linear regression model.

Predicting and Mapping Future Shoreline Retreat

Shoreline retreat can be happened due to the erosional process. Moreover, sea-level rise due to climate change can also affect the physical process in the coastal area and result in shoreline retreat (Cooper & Pilkey, 2004). Under the sea-level rise, the shoreline will retreat landward due to the absence of sand (Yoshida et al., 2014). One of the well-known methods for predicting the shoreline retreat is the *Bruun Rule*.

The Bruun Rule is a predictive method that has been widely used to respond to shoreline change due to the sea level rise (Masselink et al., 2011). This method suggested that the sea level rise can trigger the sand transport from the upper of the beach profile to the lower part of the beach so that the system remained unchanged (equilibrium state) (Cooper and Pilkey, 2004). The dune is aggraded simultaneously as the sea level rises (Kinsela et al., 2017). The loss of the sand in the upper of the beach profile will then result in the shoreline retreat. The following formula defines the Bruun Rule:

$$\boldsymbol{R = \frac{SL}{(B + h_c)}} \quad \text{..... Equation 1}$$

Where R is the shoreline recession, S is the rise in sea level, L is the width of the shoreface, B is the subaerial beach height, and h_c is the depth of the shoreface (depth closure).

As shown in **Equation 1**, the Bruun Rule highly depends on the shoreface profile since this system plays a critical role in responding to sea-level rise (Cooper & Pilkey, 2004). The *hc* can be calculated from the grain size by **Equation 2** or from the wave set of data (**Equation 3**). In addition, modelling the future shoreline retreat with a long period require the limiting depth (*hi*) as the maximum value for the depth (Hallermeier, 1981) (**Equation 4**).

$$\boldsymbol{h_c = AL^m} \quad \text{..... Equation 2}$$

$$\boldsymbol{h_c = 2Hs + 11\sigma} \quad \text{..... Equation 3}$$

$$h_i = (Hs - 0.3\sigma)T(g/5000D_{50})^{0.5} \quad \text{..... Equation 4}$$

Where h_c is the elevation (depth closure), h_i is the limiting depth, A is the grain size constant, m is the curvature of beach profile, Hs is the significant wave height, σ is the standard deviation of wave height data set, T is the average wave period, g is gravity acceleration (9.6 ms^{-2}), and D_{50} is the sediment grain-size (0.00025 m).

However, this model does not consider the uncertainty, such as climate change, the impact of the sea level rise, the model itself (Cowell et al., 2006), and oversimplifies the natural process in coastal area (Cooper & Pilkey, 2004). Due to that limitations, many researchers have adopted the new model that incorporates these uncertainties into the model by applying the Monte Carlo method. The Monte Carlo method can incorporate the key uncertainties in the shoreline recession and result in the probability distribution of shoreline recession (Wainwright et al., 2015). Instead of resulting in a single value of R (shoreline recession), the Monte Carlo will result in the R in probability value (Cowell et al., 2006). Under this model, the new shoreline recession (R) is calculated from shoreline recession due to the sea level rise (R_{sl}) and the fluctuating component of shoreline recession (R_f) by using the following formula:

$$R = R_{sl} + R_f \quad \text{..... Equation 5}$$

In this study, the Bruun Rule predicts the shoreline retreat due to the sea level rise (R_{sl}) by 2100 using 500 simulations. As the Monte Carlo method is adopted to predict the shoreline recession in a probability value, the probability value represents the probability of shoreline recession in each distance (m). This means, instead of represented in a single R_{sl} value, the shoreline recession will be defined in a probability (Cowell et al., 2006; Wainwright et al., 2015) and considers the uncertainty in the model.

Coastal Vulnerability Index (CVI) Assessment

Coastal Vulnerability Index (CVI) identifies vulnerable areas affected by coastal hazards (Pendleton et al., 2010). In this study, the CVI considers the human (proximity to human activities), topographic (presence of dune system and morphodynamics of beach), and the coastal process (rate of shoreline recession). The CVI is calculated using the scoring approach for each criterion. This score is ranging from 1 as the lowest to 3 as the highest value. In addition, the GIS-based approach is used for further analysis. The CVI is performed by using the following equation:

$$CVI = \sqrt{\frac{a\ x\ b\ x\ c\ x\ d}{4}} \quad \text{..... Equation 6}$$

Where a is human process, b is beach morphodynamic (beach type relate to energy system), c is the exposure, and d is the rate of shoreline recession. The values assigned to each category, are as follows:

Table 1 Variables and values to calculate the coastal vulnerability index.

Category	Very Low	Moderate	Very High
Variable	**1**	**2**	**3**
Morphodynamic Beach type score index (Beach_T)	Reflective	Intermediate	Dissipative/Longshore Bar and Trough
Retreat	Low shoreline retreat risk	Moderate shoreline retreat risk	High shoreline retreat risk
Exposure	Low exposure	Moderate exposure	High exposure
Human	No or little human infrastructure near the shoreline	Some infrastructure near the coast	High developed coast

4. Result

Shoreline Change

The shoreline changes in the NSI coast are presented by the Shoreline Change Envelope (SCE) value (**Figure 3a**) and the rate change in each time (**Figure 3b**). Cylinder Beach has the highest SCE value as 183.5 m change for 60 years, followed by Deadmans Beach (174.8 m). Both these beaches present the most dynamic change for the last 60 years. In contrast, Flinders and Frenchmans Beach tend to be stable and not changing much in the last 60 years.

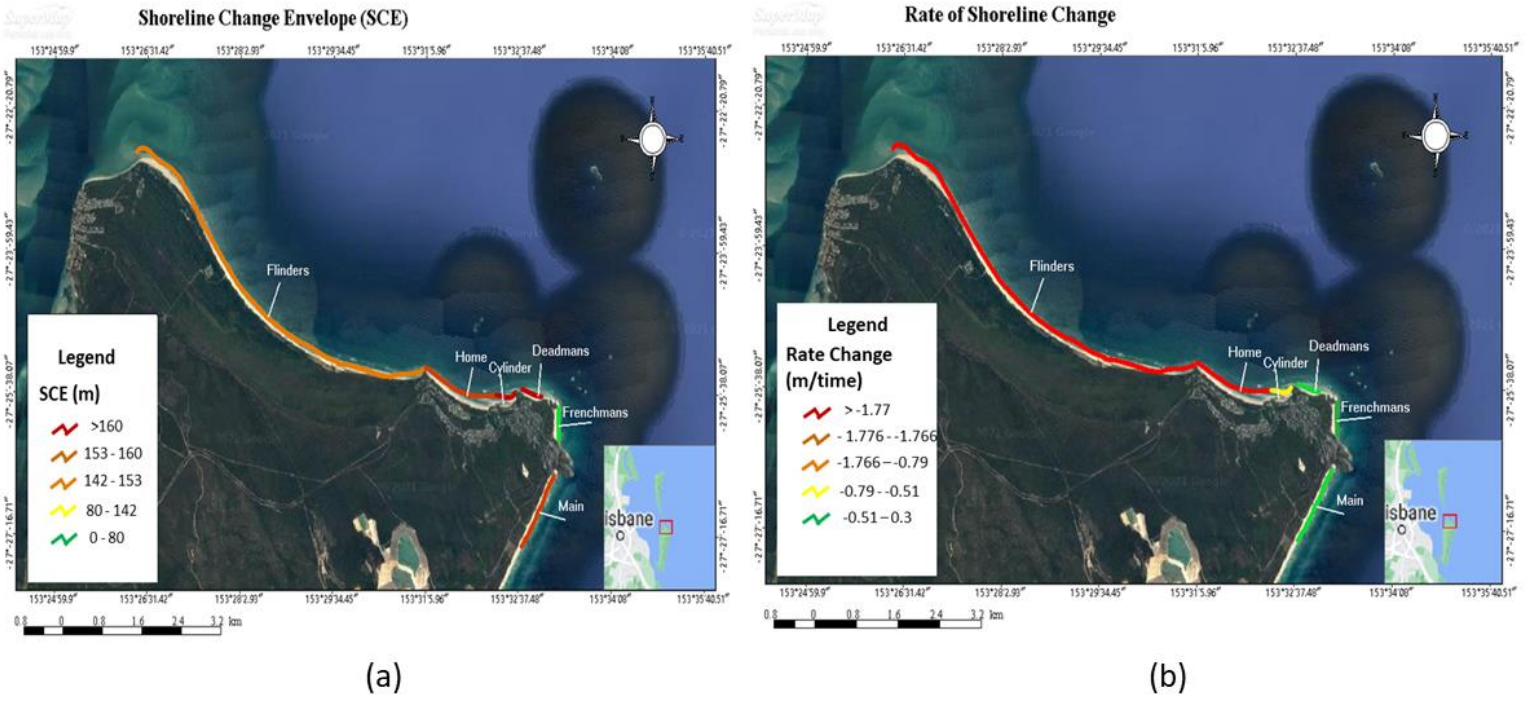

Figure 3. The result of shoreline change evaluation. (a) The change in SCE value, (b) the change rate of shoreline change.

Moreover, the tendency of shoreline change can be seen through a linear regression value (**Figure 3b**). The Flinders and Home Beach shows a significant negative value, representing the erosion and retrogradation process dominating this area (Masselink et al., 2011). Meanwhile, Deadmans Beach has the highest positive change rate, which means the accretion and progradation process dominate this zone (Masselink et al., 2011). The trend change according to the linear regression value for each beach is shown in **Figure 4**.

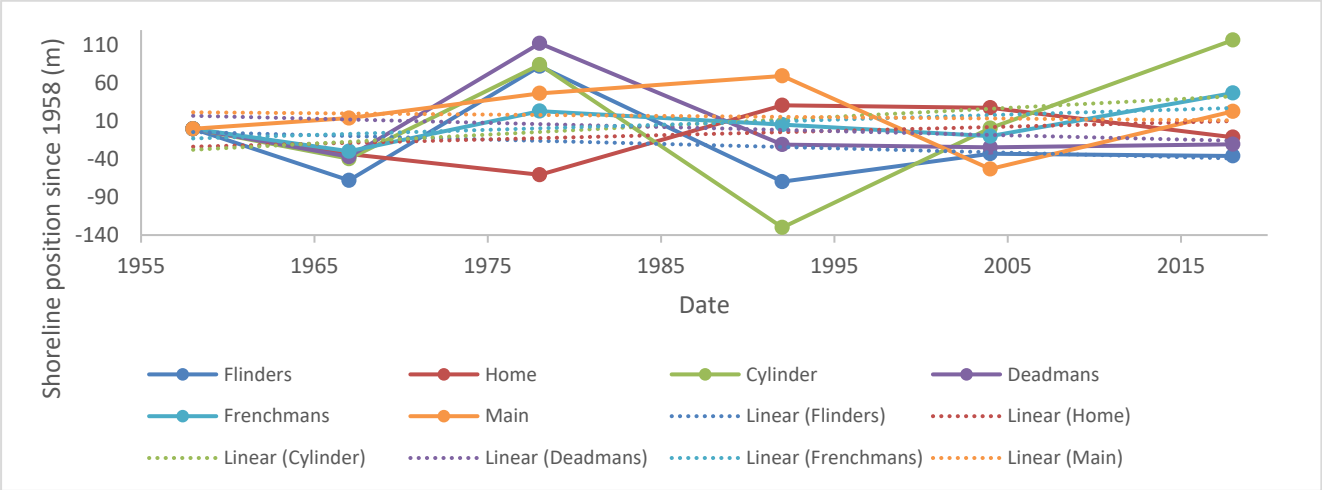

Figure 4. The historical shoreline changes in North Stradbroke Island. This chart also shows the linear regression of shoreline change in each Beach.

Future Shoreline Retreat Prediction and Map

The values for coastal recession, resulted from Bruun Rule, ranged from 18.36 to 77.35, according to a normal distribution (**Figure 5a**). This value represent the probability of the shoreline recession in different distance from sea level (Cowell et al., 2006; Wainwright et al., 2015). The trend of R_{sl} decreases as the distance of recession increase. In another way, the likelihood of a small shoreline recession is higher than the high shoreline recession. This result also shows that the probability of 15m, 48m, and 75m shoreline recession is 100% (1), 50% (0.5), and 1% (0.01) (**Figure 5b**). In addition, the probability of R_{sl} that reach 80m is 0%, or impossible to happen.

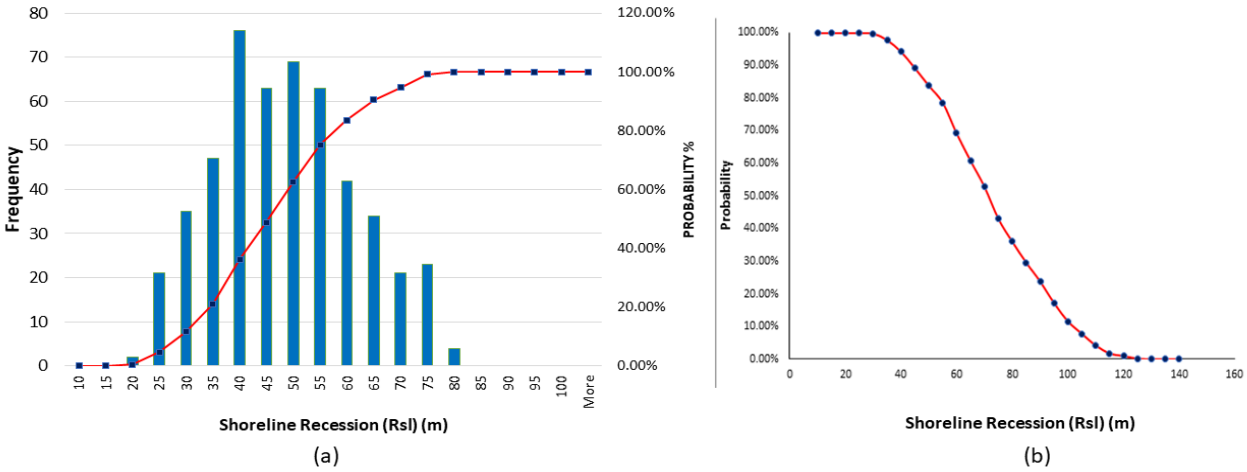

Figure 5. The result of R_sl. (a) R_sl in histogram value; (b) R_sl in probability value

Bruun Rule-Monte Carlo's result can then be used to calculate the total shoreline recession (R) (performed by using **Equation 5)**. This value considers the fluctuating component of shoreline change (R_f) in each beach and the sea level rise impact (R_sl). The shoreline recession due to sea-level rise has a similar value for each beach in each exceedance. According to this, the shoreline retreat is 48m and 75m with a 50% and 1% of probability of occurrence respectively (**Table 2**). However, the R (total retreat) value is different due to the difference of R_f in each beach. The selection of these probabilities represents the shoreline retreat simulation from the most likely until the least likely. Then, a GIS-based approach is utilized to map the potential shoreline retreat in each beach under this simulation (**Figure 6)**.

Table 2. The result of total shoreline recession (R) by 2100 calculated from R_f and R_{sl}

Variables	Flinders	Home	Cylinder	Deadmans	Frenchmans	Main
meters/year	0.001	0.077	1.228	-0.057	-0.399	0.544
cm/year	0.117	7.664	122.805	-5.654	-39.859	54.403
Average change	**-20.633**	**-15.489**	0.503	1.273	-0.785	**20.985**
Standard deviation	31.496	28.939	**65.793**	2.359	**65.810**	56.543
Shoreline fluctuations (Rf)	-52.129	-44.428	-65.289	-1.085	-66.595	-35.558
Rsl (50%) + Rf	100.129	92.428	**113.289**	49.085	**114.595**	83.558
Rsl (1%) + Rf	127.129	119.428	**140.289**	76.085	**141.595**	110.558

The beaches more affected by erosion are Frenchmans and Cylinder in cases of 50% and 1% of exceedance, resulting in a higher total shoreline recession (**Table 2**). In contrast, Deadmans Beach has the lowest R_f value (-1.085), resulting in the lowest total shoreline recession in all probabilities (**Table 2**). This means, in term of shoreline recession potential hazard, Frenchmans, and Cylinder Beach have a higher risk than others. In contrast, Deadmans Beach has the lowest potential of coastal recession in the future.

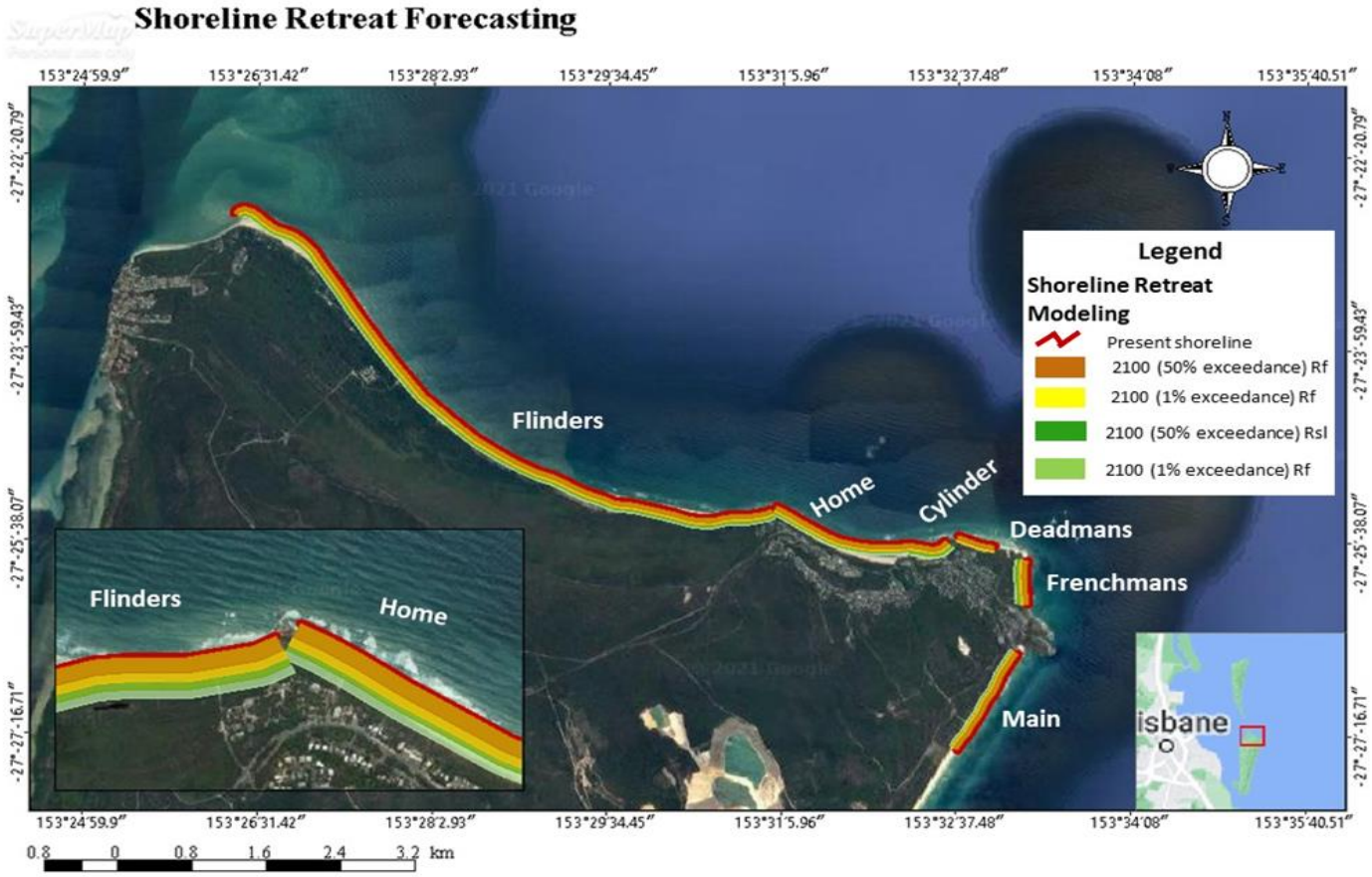

Figure 6. The result of total shoreline recession (*R*) and retreat due to sea level rise (*Rsl*) by 2100 in 50%, and 1% exceedance simulations

Respect to shoreline change, visually there is more variation in the extremes of the island corresponding to Flinders Beach and Main Beach from west to east of the island (**Figure 6**). Also, there are important variations in the blue framed are, belonging to the transition between Flinders Beach and Home beach from west to east. Coastal recession by 2100 due to *R* and *Rsl* for 1 and 50 % of exceedance is not expected to have a significant impact in Flinders beach due to the few presence of infrastructure (**Figure 6**). Similarly, it does not reach any settlement but that one located in Home beach at the boundary with Flinders Beach is the closest to the expected eroded area (**Figure 6**).

Coastal Vulnerability Index (CVI)

The high CVI in NSI tend to agglomerate in Home Beach and Cylinder Beach. Most of the CVI values in Home Beach are high, while there are only one and two boxes with high CVI values in Cylinder Beach (**Figure 7**). This pattern occurs because of the proximity of these beaches to human activities location (human settlement, campsites). In addition, the high rate of shoreline recession in these beaches also highly contribute to the high CVI value in these regions. In terms of topography, the beach profile within these beaches tends to be low, increasing exposure to coastal hazards. The low CVI value dominates the beach segment in

Flinders and Main Beach. However, moderate CVI values can be found in Flinders and Deadmans Beach. The areas with moderate CVI value in Flinders and Deadmans Beach are generally located close to human settlement, contributing to the high vulnerability of the human aspect.

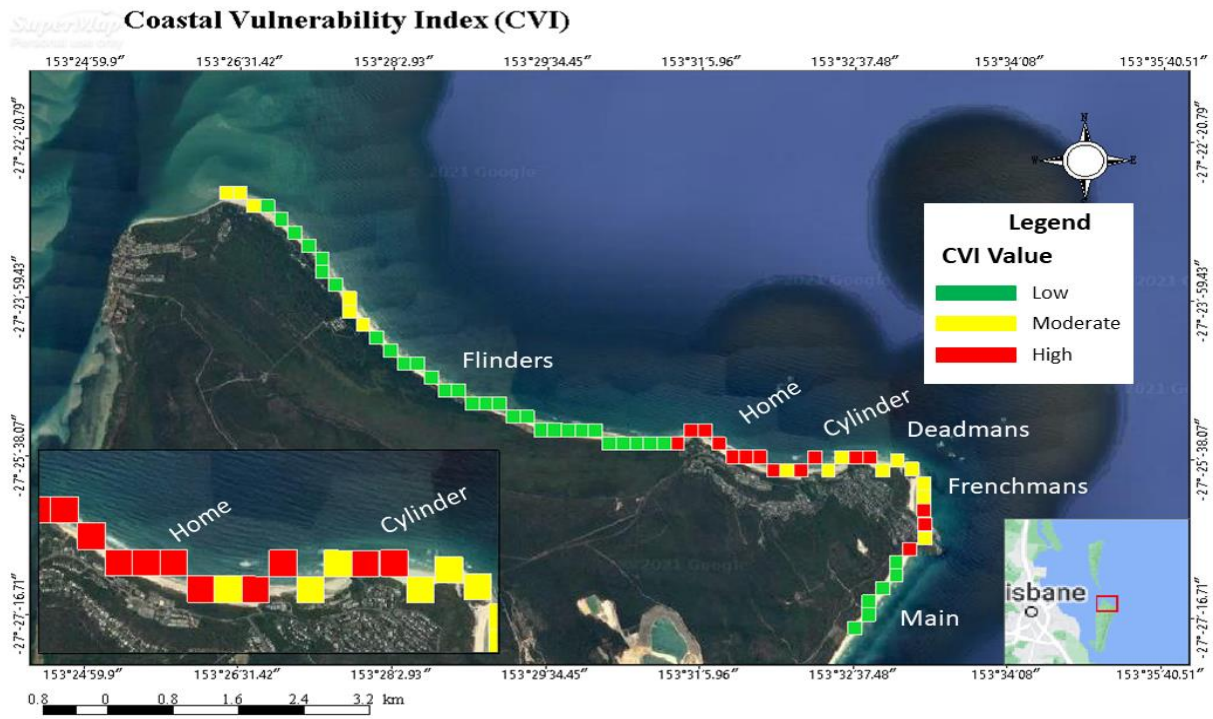

Figure 7. The coastal vulnerability index (CVI) of NSI. The CVI results from assessing human factors, shoreline recession rate, exposure, and beach morphodynamics in each beach

5. Discussion

The dynamics of shoreline change presented in **Figure 2** and **Figure 3** play essential roles for shoreline recession in NSI. The Home, Cylinder, and Frenchmans show the most dynamic change due to their high SCE value (**Figure 2a**). This dynamic has occurred under the effect of the headland bypassing process. The presence of headland in Frenchmans-Deadmans Beach (Cox et al., 2011) influences the shoreline change within this region through sediment supply and wave direction mechanism (Tong et al., 2014).

The wave in NSI move from the southeast and change its direction to northwest after hitting Main Beach. This wave system is called East Australian longshore sand transport system, which is one of the largest transport systems on the earth providing abundant sediment to the east coast by major headland bypassing (Goodwin et al., 2016). Results observed in **Table 2**, where Main Beach shows accretion state (20.98 m) and Flinders erosion state (-20.63 m) for the study period, it is interpreted as a result of such transport system.

As the wave can influence the sediment supply, it can trigger the shoreline change. Then, the headland bypassing mechanism occurs when the wave faces the headland in Frenchmans-Deadmans Beach. The case of Home beach presents a shoreline retreat of 15.49 m

as an average change of its position, it may be explained by the headland located east of Cylinder Beach, which prevent sediment supply, resulting in a prolonged recovery time (McCarroll et al., 2019; Wishaw et al., 2020).

The directional wave climate in this region drives a northward current and sediment transport from central New South Wales to the north of Fraser Island, which includes the area where NSI is located (Goodwin et al., 2016; Wishaw et al., 2021). Additionally, the fact that Cylinder and Frenchmans beaches have high standard deviation but an average change of the shoreline neglectable, may contribute to this argument by explaining that the total amount of sediment received is similar to the sediment lost, which is passed to the following beaches.

While these three beaches (Home, Cylinder, and Deadmans) are affected by headland bypassing, interestingly, the future shoreline change trend is different (**Figure 2b**). Under the parabolic effect (Tong et al., 2014), the alongshore wave and current resulted from wave refraction usually will end up by depositional process in the shadow area (Limber & Murray, 2014). The geomorphology *zetaform*, the asymmetrical deposition in the shadow area, can be found in western part Home Beach (Claudino-Sales et al., 2017). The presence *zetaform* shows the deposition process in this area. However, the total shoreline change in Home Beach shows a retrogradation (erosion) process. This means the dominant process in Home Beach is a retrogradation while the western part experiences a minor progradation (accretion). Cylinder, Deadmans, and Frenchmans gain and loose sediment almost in the same amount so that these beaches are in relatively stable condition (no progradation or retrogradation). Meanwhile, the Flinders Beach shows a retrogradation due to the erosion process dominates this area.

Cylinder and Home beaches tend to be in opposite states for most of the years; when Cylinder is in accretion, Home is in erosion and vice versa, except in 1967 that both are in erosion state. Flinders and Home beaches have a similar pattern, except in 1967 and 2015. Additionally, Main Beach that is on the extreme east side of the island, most of the time is in an accretion state which may be indicative of continuously be receiving sediment by the waves on the east coast. This phenomenon suggests that exists a continuous transport of sediment from the eastern to the western side of the coast, evidence that corresponds to Wishaw et al. (2021) and DERM (2011).

The deposition (progradation) process may dominate the sediment flux in Main Beach. Apparently, these beaches are not the source of sediment flux in northern NSI. In contrast, the sediment from other places is transported and deposited at these beaches. The effect of this depositional process still existed in Deadmans Beach, supported by the positive trend in this beach. However, the depositional process in this beach is neglectable due to the amount of sediment gained is almost equal to that loss. Due to the loss of sediment flux, the wave energy hitting headland does not have much sediment to deposit in Home Beach and Cylinder Beach. The headland also has already in an equilibrium state due to not changing much across time. This means the headland does not supply much sediment to the shadow area (Limber & Murray, 2014) in Cylinder and Home Beach. In brief, the headland by-passing in this region show an opposite headland by-passing mechanism. Understanding this physical process will then be important for the management action (William et al., 2016).

As the shoreline recession prediction relies on the R_f (fluctuating component) value, the headland bypassing mechanism significantly influences the results. In terms of coastal recession, Cylinder and Frenchmans beaches are the most affected by *Rf* and R_{sl} (**Figure 6**). This is because the R_f component is considerably significant, due to the northward sediment transport and probably due to storm events. The R_f value of Home and Cylinder Beach is the highest in NSI. The headland bypassing effect may exacerbate the shoreline recession in these beaches. In contrast, the shoreline recession in Main and Deadmans Beach is low due to the depositional process impacted by the headland bypassing.

The influence of storm events is the R_f component is supported by the wave data results (**Figure 2** and **Figure 4**) In 1978, low waves produced during calm weather conditions, transported sand to five beaches leading to accretion (highest values), excluding "Home beach" that was in an erosion state (Masselink et al., 2011). Around 1990, wave data show that there was a storm with a duration of around 800 hours and waves height of approximately 1.85 m, an event that corresponds to an erosion state (lowest values) for four beaches in 1992. Similar results were found by Griffiths et al. (2019) where storm strength was correlated to erosional events, particularly in extreme storms.

Therefore, changes observed in the R_f component might be influenced by storms as well. Coastal storms are well known for their effect on large waves and storm surges that cause inundation and damage coastal infrastructure, exacerbating coastal erosion (DERM, 2011; Tamura et al., 2019). With climate change, more storm events are expected, increasing the risk of beach erosion that could result in long term erosion and further coastal recession if the natural processes do not have enough time to restore the dune systems (DERM, 2011).

Additionally, in the future, it is expected that southeast Queensland, where NSI is located, experience around 40% reduction in northward longshore sand transport rates due to Southern Secondary Low / Southern Tasman Low events, in concert with around a 5% increase in reversed longshore sand transport for Easterly Trough Lows (ETL) events. This phenomenon will cause an overall reduction in the northward longshore sand transport, affecting the efficiency of headland bypassing events (Goodwin et al., 2016; Wishaw et al., 2020).

While the shoreline recession in this study is highly affected by the headland bypassing effect and storm events, this result leaves some shortcoming for the Bruun Rule modelling. The assumption of the Bruun Rule which does not consider the sediment flux input or output (Cooper & Pilkey, 2004), is clearly oversimplifying the actual process. The presence of headland may decrease the accuracy of the Bruun Rule result. Therefore, future research should consider this effect, especially in the study area where the effect of headland bypassing is dominant.

Moreover, the coastal vulnerability index (CVI) assessment shows three main beaches with a high coastal vulnerability index: Home Beach, Cylinder Beach, and Deadmans Beach. The physical condition (such as high rate of shoreline change (high SCE value) in the past, high shoreline recession according to the Bruun Rule prediction, and high exposure due to the low-lying beach profile) and anthropogenic condition (proximity to human settlement or campsites) cause this high CVI value. This information leads to the high priority of these beaches for the coastal management plan. This result shows another finding that headland bypassing

contributes to the coastal vulnerability result, where the beach affected by this effect may have a high vulnerability value.

According to the present results (**Figure 7**), there are no human settlements that are affected in 2100 by coastal erosion but those located in Home, Cylinder and Deadman (red pixels in the blue square) are in the limit with the area that is expected to disappear by shoreline recession. Some of these are particularly at risks due to their location in low lying lands behind the dune systems, close to intermediate beaches and very high retreat score in the CVI, which makes them vulnerable to inundation.

Thereby, NSI beaches are threatened by extreme weather events, whose effects such as storm surge and inundation can be exacerbated by future sea-level rise as well as the projected reduction in sediment transport by the East Australian longshore sand transport system. As the main recommendation, is the monitoring of the headland bypassing since it is a critical component of the sediment budget on embayed coastlines such as Home, Cylinder, Deadmans and Frenchmans beaches to develop a better understanding of this process. The outcomes will help to predict their response to wave dynamics and sea levels in the future, which may inform the management of such coastlines (McCarroll et al., 2018).

6. Conclusion

The highest shoreline retreats by 2100 under the climate change scenario will be found in Cylinder and Frenchmans Beach in cases of 50% and 1% of exceedance. This retreat is influenced by the northward sediment flux movement, storm events, and the headland bypassing process. In contrast, the shoreline recession in Main and Deadmans Beach is the lowest due to the depositional process impacted by the headland bypassing. This study also finds the high vulnerability of coastal hazards in Home Beach, Cylinder Beach, and Deadmans Beach. The high vulnerability within these beaches are mainly influenced by the presence of human settlement areas

References:

1. Burningham, H., & Miriam, F.N. (2020). Shoreline change analysis. In Jackson, D.W.T, & Short, A.D. *Sandy Beach Morphodynamics* (pp 439-460). Elsevier. http://dx.doi.org/10.1016/B978-0-08-102927-5.00019-9
2. Cooper, J.A.G., Pilkey, O.H. (2004). Sea-level rise and shoreline retreat: time to abandon the Bruun Rule. *Global and Planetary Change, 43*, pp. 157–171
3. Cowell, P.J., Thom, B.G., Jones, R.A., Everts, C.H., & Simanovic, D. (2006) . Management of Uncertainty in Predicting Climate-Change Impacts on Beaches. *Journal of Coastal Research, 22*(1), pp. 232-245
4. Cox, M.E., James, A., Hawke, A., Specht, A., Raiber, M. & Taulis, M. (2011). North Stradbroke Island 3d Hydrology: Surface Water Features, Settings and Groundwater Links. Proceedings of The Royal Society of Queensland

5. Dean, R.G. (1977). *Equilibrium beach profiles: U.S. Atlantic and Gulf coasts*. Department of Civil Engineering, University of Delaware, Technical Report No. 12, 45 pp.
6. Deepika, B., Avinash, K., Jayappa, K.S. (2013). Shoreline change rate estimation and its forecast: remote sensing, geographical information system and statistics-based approach. *International Journal of Environment Science Technology*. https://doi.org/10.1007/s13762-013-0196-1
7. den Boer, E.L., Suntoyo, Oele, A.C. (2018). Determination of shoreline change along the East-Java coast, using Digital Shoreline Analysis System. *MATEC Web of Conferences 177*. https://doi.org/10.1051/matecconf/201817701022
8. Goodwin, I. D., Mortlock, T. R., & Browning, S. (2016). Tropical and extratropical-origin storm wave types and their influence on the East Australian longshore sand transport system under a changing climate. Journal of geophysical research. Oceans, 121(7), 4833-4853. https://doi.org/10.1002/2016JC011769
9. Hallermeier, R.J. (1981). *Seaward limit of significant sand transport by waves: an annual zonation for seasonal profiles*. Coastal Engineering Research Center Fort Belvoir Va.
10. Huang, W.P., Hsu, J.C., Chen, C.S., & Ye, C.J. (2018). The Study of the Coastal Management Criteria Based on Risk Assessment: A Case Study on Yunlin Coast, Taiwan, Water, vol. 10
11. Kinsela, M.A., Morris, B.D., Daley, M.J.A. and Hanslow, D.J. (2016). A Flexible Approach to Forecasting Coastline Change on Wave-Dominated Beaches. In: Vila-Concejo, A.; Bruce, E.; Kennedy, D.M., and McCarroll, R.J. (eds.), Proceedings of the 14th International Coastal Symposium (Sydney, Australia). Journal of Coastal Research, Special Issue, No. 75, pp. 952-956
12. Kinsela, M., Morris, B., Linklater, M. and Hanslow, D. (2017). Second-Pass Assessment of Potential Exposure to Shoreline Change in New South Wales, Australia, Using a Sediment Compartments Framework. *Journal of Marine Science and Engineering*, *5*(4): 61.
13. Limber, P.W., & Murray, A.B. (2014). Unraveling the dynamics that scale cross-shore headland relief on rocky coastlines: 2. Model predictions and initial tests. *Journal of Geophysical Research: Earth Surface*, *119*, pp. 874–891, https://doi.org/doi:10.1002/2013JF002978
14. McCarroll, R. J., Masselink, G., Valiente, N. G., Scott, T., King, E. V., & Conley, D. (2018). Wave and Tidal Controls on Embayment Circulation and Headland Bypassing for an Exposed, Macrotidal Site. Journal of marine science and engineering, 6(3), 94. https://doi.org/10.3390/jmse6030094
15. McCarroll, R. J., Masselink, G., Wiggins, M., Scott, T., Billson, O., Conley, D. C., & Valiente, N. G. (2019). High-efficiency gravel longshore sediment transport and headland bypassing over an extreme wave event. Earth surface processes and landforms, 44(13), 2720-2727. https://doi.org/10.1002/esp.4692
16. Masselink, G., Hughes, M.G., & Knight, J. (2011). *Coastal Process & Geomorphology: Second Edition*. Routledge

17. Mehvar, S., Filatova, T., Dastgheib, A. Steveninck, E.R., & Ranasinghe, R. (2018). Quantifying Economic Value of Coastal Ecosystem Services: A Review. *Journal of Marine Science & Engineering, 6, 5*. https://doi.org/10.3390/jmse6010005
18. Pendleton, E.A., Barras, J.A., Williams, S.J., Twichell, D.C. (2010). *Coastal vulnerability assessment of the Northern Gulf of Mexico to sea-level rise and coastal change*. U.S. Geological Survey Open-File Report 2010-1146.
19. Saravanan, S., Parthasarathy, K.S.S., Vishnuprasath, S.R. (2019). Monitoring Spatial and Temporal Scales of Shoreline Changes in the Cuddalore Region, India. *Coastal Zone Management*, pp. 99-112. https://doi.org/10.1016/B978-0-12-814350-6.00004-5
20. Claudino-Sales, V.; Wang, P., and Carvalho, A.M., (2017). Interactions between various headlands, beaches, and dunes along the coast of Ceara´ State, Northeast Brazil. *Journal of Coastal Research*
21. Wainwright, D. J., Ranasinghe, R., Callaghan, D. P., Woodroffe, C. D., Jongejan, R., Dougherty, A. J., Rogers, K. & Cowell, P. J. (2015). Moving from deterministic towards probabilistic coastal hazard and risk assessment: development of a modelling framework and application to Narrabeen Beach, New South Wales, Australia. *Coastal Engineering, 96*, pp. 92-99
22. Whitlow, R. (2000). *The Geology and Geomorphology of North Stradbroke Island: An investigation into the nature, morphology and origins of dune landforms and associated water features*. Report by TriMap Pty Ltd Geoscientific Consulting
23. Wishaw, D., Leon, J. X., Barnes, M., & Fairweather, H. (2020). Tropical Cyclone Impacts on Headland Protected Bay. Geosciences (Basel), 10(5), 190. https://doi.org/10.3390/geosciences10050190
24. Wishaw, D., Leon, J., Fairweather, H., & Crampton, A. (2021). Influence of wave direction sequencing and regional climate drivers on sediment headland bypassing. Geomorphology (Amsterdam, Netherlands), 383, 107708. https://doi.org/10.1016/j.geomorph.2021.107708
25. Williams, A., Rangel-Buitrago, N.G., Pranzini, E., & Anfuso, G. (2017). The management of coastal erosion, *Ocean & Coastal Management*, http://dx.doi.org/10.1016/j.ocecoaman.2017.03.022
26. Yoshida, J., Udo, K., Takeda, Y., Mano, A. (2014). Framework for proper beach nourishment as adaptation to beach erosion due to sea level rise. In: Green, A.N. and Cooper, J.A.G. (eds.), Proceedings 13th International Coastal Symposium (Durban, South Africa), Journal of Coastal Research, Special Issue No. 70, pp. 467-472, ISSN 0749-0208.
27. Griffiths, D., House, C., Rangel-Buitrago, N. & Thomas, T. (2019). An assessment of areal and transect-based historic shoreline changes in the context of coastal planning. Journal of Coastal Conservation, 23, 315–330. https://doi.org/10.1007/s11852-018-0661-6